

See discussions, stats, and author profiles for this publication at: <https://www.researchgate.net/publication/231223242>

# Comprehensive Molecular Motion Capture for Sphingomyelin by Site-Specific Deuterium Labeling

ARTICLE *in* BIOCHEMISTRY · SEPTEMBER 2012

Impact Factor: 3.02 · DOI: 10.1021/bi3009399 · Source: PubMed

---

CITATIONS

15

---

READS

27

9 AUTHORS, INCLUDING:



Tohru Oishi

Kyushu University

131 PUBLICATIONS 2,374 CITATIONS

SEE PROFILE



Michio Murata

Osaka University

224 PUBLICATIONS 7,476 CITATIONS

SEE PROFILE

# Comprehensive Molecular Motion Capture for Sphingomyelin by Site-Specific Deuterium Labeling

Nobuaki Matsumori,<sup>\*,†</sup> Tomokazu Yasuda,<sup>†</sup> Hiroki Okazaki,<sup>†</sup> Takashi Suzuki,<sup>†</sup> Toshiyuki Yamaguchi,<sup>†,‡</sup> Hiroshi Tsuchikawa,<sup>†</sup> Mototsugu Doi,<sup>†</sup> Tohru Oishi,<sup>§</sup> and Michio Murata<sup>\*,†,‡</sup>

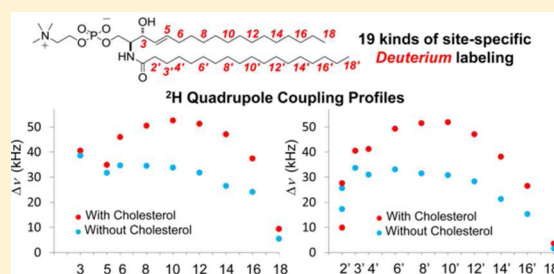
<sup>†</sup>Department of Chemistry, Graduate School of Science, Osaka University, Toyonaka, Osaka 560-0043, Japan

<sup>‡</sup>ERATO, Lipid Active Structure Project, Japan Science and Technology Agency, Toyonaka, Osaka 560-0043, Japan

<sup>§</sup>Department of Chemistry, Graduate School of Sciences, Kyushu University, Higashi-ku, Fukuoka 812-8581, Japan

## S Supporting Information

**ABSTRACT:** Lipid rafts have attracted much attention because of their significant functional roles in membrane-associated processes. It is thought that sphingomyelin and cholesterol are essential for forming lipid rafts; however, their motion characteristics are not fully understood despite numerous studies. Here we show accurate local motions encompassing an entire sphingomyelin molecule, which were captured by measuring quadrupole splittings for 19 kinds of site-specifically deuterated sphingomyelins (that is, *molecular motion capture* of sphingomyelin). The quadrupole splitting profiles, which are distinct from those reported from perdeuterated sphingomyelins or simulation studies, reveal that cholesterol enhances the order in the middle parts of the alkyl chains more efficaciously than at the shallow positions. Comparison with dimyristoylphosphocholine bilayers suggests that cholesterol is deeper in sphingomyelin bilayers, which likely explains the so-called umbrella effect. The experiments also demonstrate that (i) the C2'–C3' bond predominantly takes the gauche conformation, (ii) the net ordering effect of cholesterol in sphingomyelin bilayers is not larger than that in phosphatidylcholine bilayers, (iii) cholesterol has no specific preference for the acyl or sphingosine chain, (iv) the acyl and sphingosine chains seem mismatched by about two methylene lengths, and (v) the motion of the upper regions of sphingomyelin chains is less temperature dependent than that of lower regions probably due to intermolecular hydrogen bond formation among SM molecules. These insights into the atomic-level dynamics of sphingomyelin provide critical clues to understanding the mechanism of raft formation.



To date, numerous studies have been conducted experimentally and theoretically to reveal the order of phospholipids in membranes and the ordering effect of cholesterol (Chol). In particular, solid-state  $^2\text{H}$  NMR spectroscopy has frequently been used for this purpose because it lends itself to noninvasive investigation of the order and mobility of acyl chains in lipid bilayers.<sup>1</sup> These  $^2\text{H}$  NMR measurements provide quadrupole splitting ( $\Delta\nu$ ) of chain deuterons located in lipid bilayers, which allows us to determine the segmental order parameters. However, previous  $^2\text{H}$  NMR studies largely suffered from severe overlapping of quadrupole splittings inherent in perdeuterated acyl chains,<sup>2–4</sup> which can lead to misassignment of deuterium signals. Another potential concern in using multideuterated lipids is that the accumulated deuterium isotope effects alter the chemical and physical properties of their lipid bilayers; for example, chain melting temperatures are known to decrease as a consequence of the perdeuteration of acyl chains.<sup>5</sup> To avoid these concerns inherent in multideuterated lipids as well as to gain accurate local dynamics information on the lipid molecule, selectively deuterated lipids are particularly desired.

Among the membrane lipids, selective deuteration of sphingomyelin (SM) is of special interest because of its

essential role in the formation of lipid rafts.<sup>6</sup> Until now, 2',2'- $d_2$ -, 3',3'- $d_2$ -, 3,4,5- $d_3$ -, and 3- $d$ -N-palmitoyl SMs have been reported;<sup>2,7</sup> however, site-specific deuteration of the long-chain regions of SM has not yet been reported. In particular, either selective or multiple deuteration has never been achieved for the sphingosine methylene chain. In this study, we successfully synthesized 19 kinds of site-specifically deuterated SMs (Chart 1), which allowed us to accurately capture the segmental motions encompassing the whole SM molecule (that is, *molecular motion capture* of SM). Consequently, the effect of Chol on the SM membrane could be evaluated in detail.

## MATERIALS AND METHODS

Full synthetic procedures for the deuterated SSMs are described in the Supporting Information.

**Sample Preparation for  $^2\text{H}$  NMR.** Because commercially available semisynthetic SSM is a mixture of epimers at C3 of sphingosine, we purified SSM from bovine brain SM (Avanti

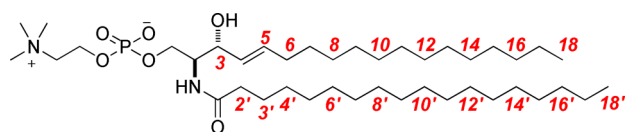
Received: July 14, 2012

Revised: September 27, 2012

Published: September 27, 2012



**Chart 1. Structure of Site-Specifically Deuterated *N*-Stearoyl Sphingomyelin (SSM)<sup>a</sup>**



<sup>a</sup>Each numbered position was deuterium labeled. A total of 19 kinds of deuterium-labeled SSM were prepared to capture the motion of SSM in membranes.

Polar Lipids) by reverse-phase HPLC.<sup>8</sup> For preparation of SSM membrane, a mixture of 10.5  $\mu$ mol of purified SSM and 10.5  $\mu$ mol of deuterated SSM was dissolved in MeOH–CHCl<sub>3</sub>. For SSM–Chol sample, a mixture of 10.5  $\mu$ mol of purified SSM, 10.5  $\mu$ mol of deuterated SSM, and 21.0  $\mu$ mol of Chol (Nacalai Tesque) was dissolved in the solvent. The solvent was removed in vacuo for at least 12 h. The dried membrane film was hydrated with ca. 1 mL of water and vigorously vortexed (Vortex-Genie 2 or Branson 1510) at a temperature of 65 °C to make multilamellar vesicles. After being freeze–thawed three times, each suspension was lyophilized, rehydrated with deuterium-depleted water (Isotec Inc.) to be 50% moisture (w/w), and freeze–thawed several times. Then each sample was transferred into a 5 mm glass tube (Wilmad), which was sealed with epoxy glue.

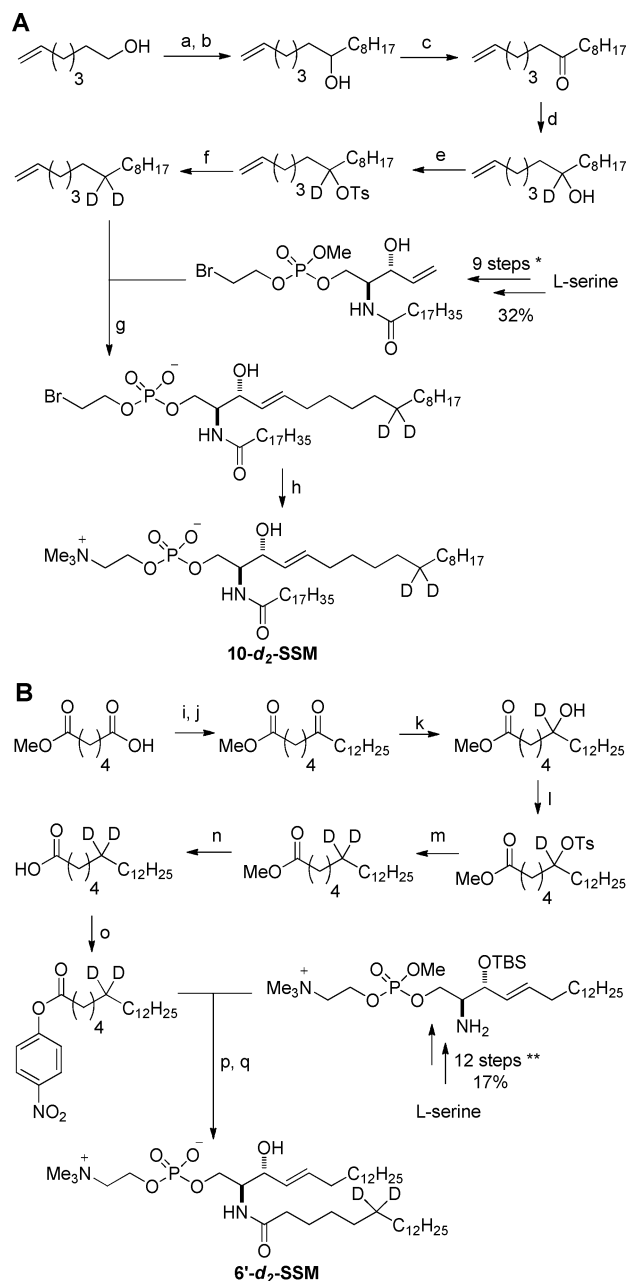
**<sup>2</sup>H NMR Measurements.** <sup>2</sup>H NMR spectra were recorded on a 300 MHz CMX300 spectrometer (Chemagnetics, Varian, Palo Alto, CA) with a 5 mm <sup>2</sup>H static probe (Otsuka Electronics, Osaka, Japan) using a quadrupolar echo sequence.<sup>9</sup> The 90° pulse width was 2  $\mu$ s, interpulse delay was 30  $\mu$ s, and repetition rate was 0.5 s. The sweep width was 200 kHz, and the number of scans was around 100 000.

## RESULTS AND DISCUSSION

**Preparation of Site-Specifically Deuterated SSMs and Their <sup>2</sup>H Quadrupole Splittings.** As shown in Chart 1, we selected *N*-stearoyl SM (SSM) because it is known to be the most abundant SM constituent in bovine brain<sup>10</sup> and to recruit some raft-specific proteins more efficiently than other SMs with shorter acyl chains.<sup>11</sup> A total of 19 kinds of site-specifically deuterated SSMs were synthesized as shown in Schemes S1–S8 (Supporting Information) by modification of previously reported procedures.<sup>12–14</sup> Scheme 1 shows examples of the synthesis for SSMs deuterated at sphingosine and acyl chains. Briefly, for synthesis of 10-*d*<sub>2</sub>-SSM (Scheme 1A), 7-deuterated pentadecene was prepared by reduction of the ketone with NaBD<sub>4</sub>, conversion of the resulting secondary alcohol to the tosylate, and treatment with LiAlD<sub>4</sub>. Then, the olefin metathesis reaction with the allyl alcohol, which was synthesized from *L*-serine according to a previous report,<sup>12</sup> provided the precursor of 10-*d*<sub>2</sub>-SSM (Scheme 1A). For synthesis of 6'-*d*<sub>2</sub>-SSM, 6-deuterated stearic acid was prepared by reducing the ketone with NaBD<sub>4</sub> (Scheme 1B). Coupling with sphingosine, which was synthesized from *L*-serine based on previous reports,<sup>12–14</sup> provided protected 6'-*d*<sub>2</sub>-SSM (Scheme 1B). Full synthetic procedures for the deuterated SSMs except 3-*d*-SSM and 10'-*d*<sub>2</sub>-SSM, which were prepared as previously reported,<sup>15</sup> are described in the Supporting Information.

With the labeled SSMs in hand, we measured their <sup>2</sup>H NMR spectra and determined the quadrupole coupling values ( $\Delta\nu$ ) in membrane form in the presence and absence of 50 mol % Chol

**Scheme 1. Examples of Synthesis of Sphingomyelins Deuterated at Sphingosine (A) and Acyl Chain (B)<sup>a</sup>**



<sup>a</sup>Conditions: (a) IBX, DMSO, rt, 4 h; (b) CH<sub>3</sub>(CH<sub>2</sub>)<sub>7</sub>MgBr, Et<sub>2</sub>O, rt, 18 h, 75% (2 steps); (c) SO<sub>3</sub>–Py, Et<sub>3</sub>N, DMSO, CH<sub>2</sub>Cl<sub>2</sub>, rt, 14 h, 83%; (d) NaBD<sub>4</sub>, MeOH–CHCl<sub>3</sub>, 0 °C, 2 h, 96%; (e) TsCl, Et<sub>3</sub>N, DMAP, CH<sub>2</sub>Cl<sub>2</sub>, rt, 45 h, 80%; (f) LiAlD<sub>4</sub>, Et<sub>2</sub>O, rt, 5 h, 86%; (g) Grubbs second, CH<sub>2</sub>Cl<sub>2</sub>, reflux, 2 h, 51%; (h) NMe<sub>3</sub> aq, MeOH, rt, 17 h, 43%; (i) (COCl)<sub>2</sub>, toluene, rt, 1 h; (j) CH<sub>3</sub>(CH<sub>2</sub>)<sub>11</sub>MgBr, CuI, THF, –78 °C 2 h, 61% (2 steps); (k) NaBD<sub>4</sub>, MeOH–CHCl<sub>3</sub>, 0 °C, 2 h, 93%; (l) TsCl, Et<sub>3</sub>N, DMAP, CH<sub>2</sub>Cl<sub>2</sub>, rt, 45 h, 74%; (m) NaBD<sub>4</sub>, DMSO, 80 °C, 14 h, 54%; (n) NaOH aq, MeOH–THF, 60 °C, 2 h, quant; (o) DCC, *p*-nitrophenol, THF, rt, 18 h, 80%; (p) Et<sub>3</sub>N, DMAP, THF, rt, 17 h; (q) TBAF, THF, rt, 17 h, 63% (2 steps). \*Reference 12. \*\*References 12–14

(Figure 1). Because the phase transition temperature of a pure SSM membrane is 44 °C,<sup>16</sup> the measurements were carried out at 45 °C. We also examined 12'-*d*<sub>2</sub>-SSM membranes containing 33 mol % Chol instead of 50 mol % and confirmed that the

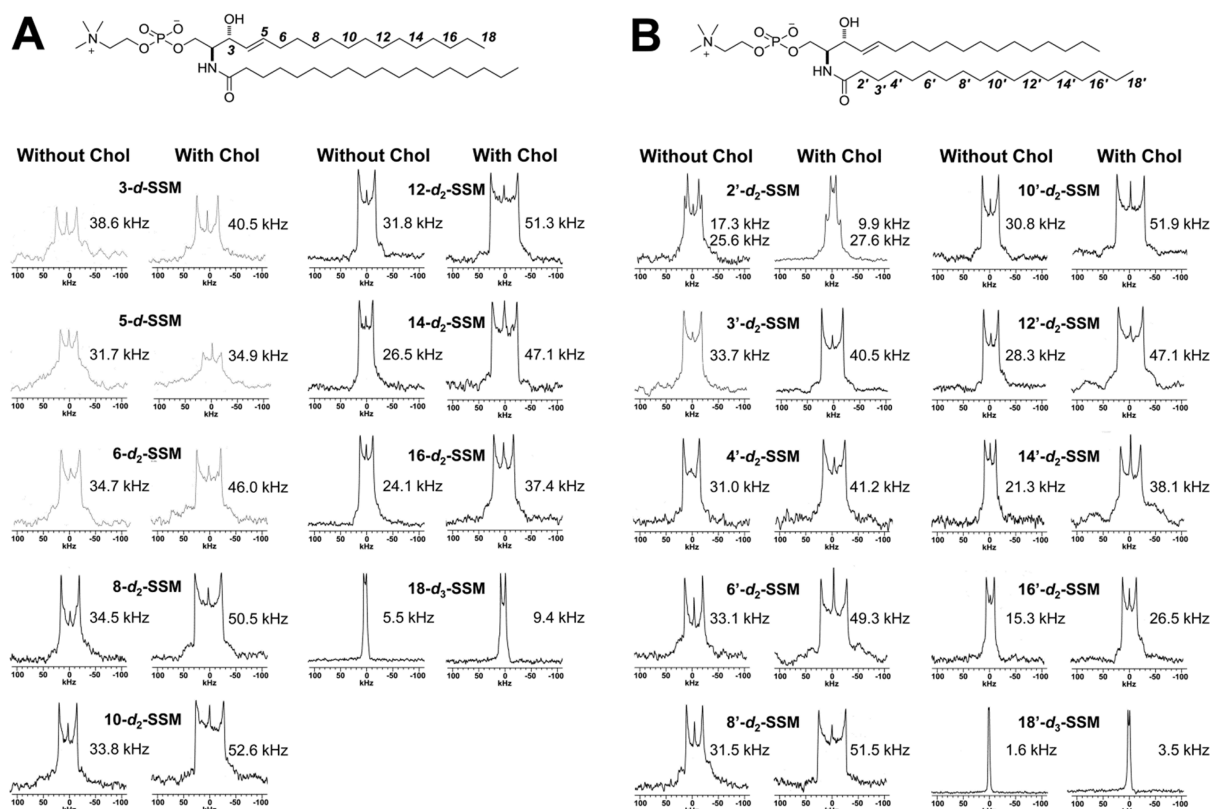


**Figure 1.**  $^2\text{H}$  NMR spectra of deuterated SSM bilayers in the presence and absence of 50 mol % Chol at 45 °C. The sphingosine chain (A) or acyl chain (B) is site-selectively deuterated. To conserve the amount of deuterated SSMs, we mixed unlabeled SSM that was isolated from a bovine brain-derived SM mixture by HPLC.<sup>8,10</sup>

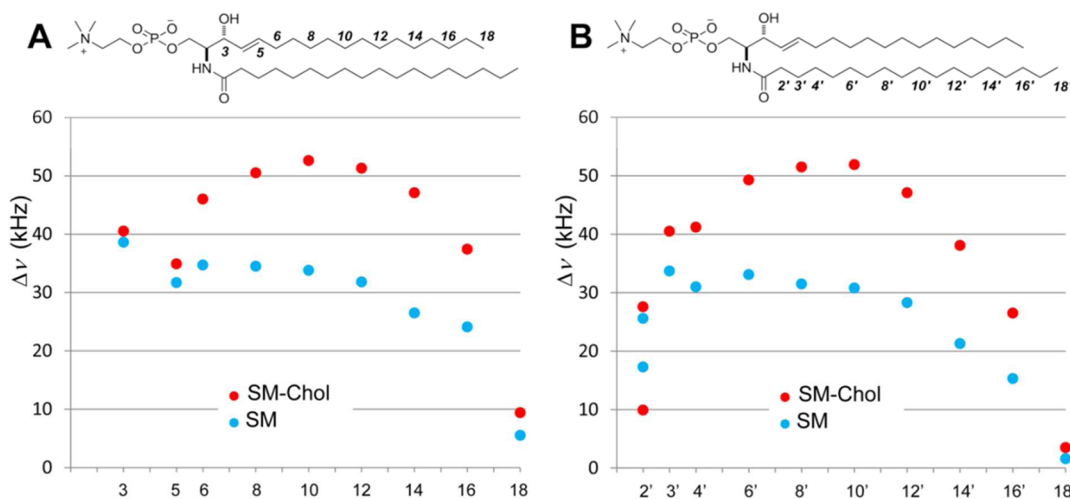


**Figure 2.** Quadrupole splitting profiles obtained from SSM that has been site-specifically deuterium-labeled on the sphingosine (A) and stearoyl (B) chains. Data were obtained in the absence (blue circles) and presence (red ones) of 50 mol % Chol at 45 °C.

quadrupole splitting data are essentially identical between 33 and 50 mol % Chol. As is evident from Figure 1, 2'-d<sub>2</sub>-SSM gives rise to two pairs of doublets both in the presence and absence of Chol, whereas other selectively deuterated SSMs show a single pair. The magnitude of quadrupole splitting depends both on average segment orientation and on the degree of motional averaging. Since the two deuterium atoms on C2' undergo the same motional averaging, the observation suggests that the acyl chain predominantly kinks at the C2'–C3' bond and the two C–D bonds on C2' take different average orientations with respect to the axis of rotational

averaging, thus giving two pairs of doublet signals.<sup>2,17</sup> Notably, the difference between the two quadrupole splittings at the C2' position is larger in the presence of Chol (8.3 kHz in the absence of Chol and 17.7 kHz in its presence), which suggests that Chol enhances the population of the gauche conformation at the C2'–C3' bond and/or changes the average angle between the rotation axis and the C2'–C3' bond.

Figure 2 shows the quadrupole splitting profiles of SSM in the absence and presence of Chol at 45 °C, from which we clearly see that Chol efficaciously enhances the order in the middle portions of both sphingosine and acyl chains. However,



its effect is much smaller at the shallow parts of SSM, as seen at C3 and C5 of sphingosine (Figure 2A) and C3' and C4' of the acyl chain (Figure 2B). The order parameters at C10 and C10' in the presence of Chol were calculated to be 0.40, which is close to the maximum value of 0.5, suggesting that chain fluctuation is significantly suppressed in the middle regions of both alkyl chains.

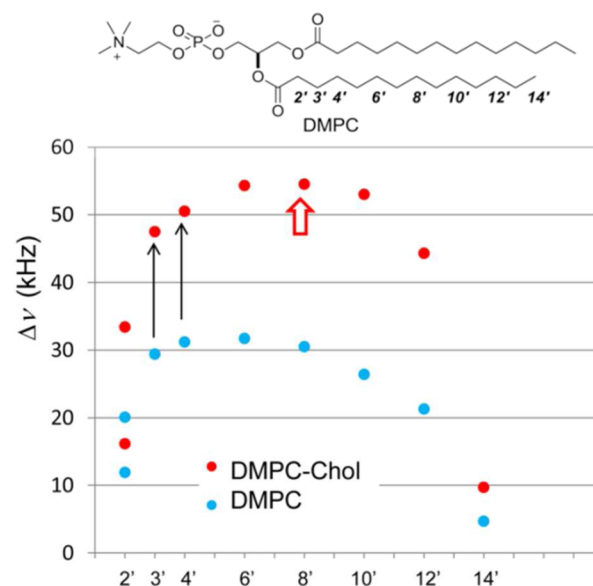
It was reported that lipid alkyl chains in bilayers undergo rapid gauche–trans isomerization, and the chain order parameters (i.e., quadrupole splitting values) are qualitatively correlated with trans populations of the C–C bonds.<sup>18</sup> Since the rigid alicyclic skeleton of Chol increases the trans percentage of the C–C bonds,<sup>18</sup> straightens the chain, and effectively enhances the order,<sup>19,20</sup> the profiles in Figure 2 may imply that Chol's alicyclic skeleton is preferentially located in the middle portions of the SSM hydrocarbon chains.

Figure 2B also shows that the presence of Chol less increases the order in the upper chain region than that in the middle positions. This may be interpreted, albeit qualitatively, as follows. In our previous paper that reported the conformation of SM in membrane environment,<sup>15</sup> the amide plane of SM is likely to be parallel to the membrane plane, probably because the hydrogen bond formation with neighboring SM molecules. On the other hand, in the presence of Chol, the middle-chain region should predominantly take a relatively straight orientation with its axis perpendicular to the membrane surface. That means that the chain segment between the amide and the middle chain must be bent. As described above, the C2'–C3' bond predominantly takes a gauche conformation, but it may not enough to relieve the strain, and the other C–C bonds (i.e., from C3' to middle chain) also take part in the gauche conformation. This would increase the gauche population of the C–C bonds between the amide and the middle chain, resulting in the smaller splitting in this region. This effect, along with the aforementioned ordering effect of Chol in the middle chain, could influence the location of the splitting maximum along the chain. A more detailed discussion on the correlation between the order profile and the depth of Chol is described later.

Here it should be emphasized that this study is the first to reveal the <sup>2</sup>H NMR profiles in the sphingosine chain of SM (Figure 2A) because neither selective nor multiple deuteration had been achieved for the sphingosine methylene chain before this study. In addition, we must stress that our characteristic <sup>2</sup>H NMR profile of the SM acyl chain (Figure 2B) is different from those obtained from SMs that bear perdeuterated acyl chains<sup>2,3,21</sup> because in previous studies the overlapped doublet signals from the perdeuterated acyl chains were assigned by assuming that the quadrupole splitting decreases monotonically from the lipid–water interface toward the terminal.<sup>2–4</sup> A comparison of quadrupole splitting profiles of SM acyl chain between previous report<sup>3</sup> and current data is shown in Figure S4 of the Supporting Information, which clearly demonstrates the necessity of our comprehensive and selective deuteration strategy. Our results, therefore, may suggest that previous quadrupole splitting profiles obtained from perdeuterated lipids should be reexamined.

**Comparison with DMPC.** Then we compared Chol's ordering effects on SSM with those on diacylglycerophosphocholines (PCs). The only available experimental data on segmental quadrupole splittings for PCs are, to our knowledge, those of dimyristoylphosphocholine (DMPC), which were obtained by Oldfield et al. using site-specifically deuterated

DMPC (Figure 3).<sup>22</sup> Comparison of the quadrupole splittings in the acyl chains of SSM and DMPC (Figures 2B and 3) shows



**Figure 3.** Reported quadrupole splittings of *sn*2-acyl chain of DMPC in the presence and absence of 30 mol % Chol.<sup>22</sup> The acyl chain was site-specifically <sup>2</sup>H labeled. Thin arrows indicate the order enhancement by Chol, and thick red arrow shows the maximum position in the Chol-containing membrane.

that Chol enhances the orders of the shallow region (C3' and C4') more effectively in DMPC than in SSM bilayers and that the position with the maximum quadrupole splitting of Chol-containing bilayers is deeper in SSM than in DMPC membrane by about two methylene groups (C8' for DMPC–Chol in Figure 3 and C10' for SSM–Chol in Figure 2B). These findings may suggest that the rigid alicyclic rings of Chol are located deeper in SSM than in DMPC bilayers. However, of major concern here is the validity of the discussion that the shape of order profile reflects the location of steroid rings. Based on the aforementioned notion that the rigid Chol's rings increase the trans population and enhance the order in the middle chain,<sup>18</sup> it is not far-fetched to connect the order profile and Chol's location. Here, comparison with the effect of different Chol locations on simulated splittings might be helpful to interpret these observations. A simulation study showed that shallowly located sterol molecule increases order parameters of upper chain effectively and shifts the order profile to the upper region,<sup>23</sup> which seems supportive of the correlation between the order profile and location of steroid rings.

To further support the deeper location of Chol in SSM membrane, we inspected the reported electron density profiles for SSM–Chol and DMPC–Chol membrane systems obtained from X-ray and neutron diffraction experiments (see Figures S1–S3 in the Supporting Information),<sup>24–26</sup> and the comparison suggests that the distance between the membrane headgroup and Chol rings can be longer in SSM–Chol than in DMPC–Chol membranes (for more detailed discussion, refer to the Supporting Information). The location of Chol being deeper in SSM than in DMPC membrane seems also reproduced by a simulation study,<sup>27</sup> which showed that in the SM–Chol bilayer the OH group of Chol locates, on average, 0.8 Å lower in the interface than in the DMPC–Chol bilayer because H-bonding anchors the OH group of Chol in the lower

regions of the SSM–Chol bilayer interface. Overall, these discussions seem to support the deeper location of Chol in SSM membranes than in DMPC; however, there is a significant concern about the comparison between SSM and DMPC membranes because of the difference in acyl chain length. Therefore, it would be interesting to compare also the distances from Chol rings to the head groups in PC membrane that shares the same acyl chain as SSM. In fact, comparison of the quadrupole splittings of SSM with those of palmitoylstearylphosphocholine (PSPC) is now in progress.

It is well-known that SM strongly shields Chol from unfavorable contact with the water layer (the so-called umbrella effect).<sup>28</sup> The umbrella effect was experimentally shown by the observation that the desorption of Chol caused by  $\beta$ -cyclodextrin is slower from SM membrane as compared to that from PC membrane.<sup>29</sup> This effect has been explained by the idea that Chol molecules are covered with SM choline groups. For instance, a simulation study suggested that a charge-dipole interaction between the choline ammonium cation of SM and the OH group in Chol plays an important role in the capping on Chol molecule.<sup>30</sup> In the model, however, Chol should come close to the upper region of membrane to interact with the choline ammonium. The present data, by contrast, suggest that the origin of the umbrella effect may be the deeper immersion of Chol in the SM bilayers, which prevents contact with the water layer. This seems consistent with the above  $\beta$ -cyclodextrin-mediated sterol desorption experiment<sup>29</sup> because the deeper location of Chol in SM bilayers should retard its removal by  $\beta$ -cyclodextrin. Then, why is Chol preferentially distributed in deeper regions of SM bilayers? It is well-known that the hydroxy and amide groups of SM involve in the formation of intermolecular hydrogen bonds in SM membranes,<sup>31</sup> which would suggest the formation of a hydrogen bond network among SM molecules. This hydrogen bond network, which is not formed in PC membranes due to the lack of hydrogen bond donors, might push Chol downward into the SM membrane core or prevent Chol from rising up.

Figures 2B and 3 also suggest that the net ordering effect of Chol is not larger in SSM membranes than in DMPC membranes. It has been proposed that the nature of the SM–Chol interaction is more attractive when compared with the interactions of Chol with other lipids, and the ability of Chol to specifically interact with SM is a driving force in liquid-ordered phase formation in SM/Chol bilayers.<sup>20,32</sup> Our quadrupole splitting data, however, could not support the existence of a specific interaction between Chol and SM.<sup>33</sup>

**Comparison of Quadrupole Splitting Profiles between Sphingosine and Acyl Chains.** Next, we compared the motion characteristics of the acyl and sphingosine chains, as shown in Figure 4, where the quadrupole splitting profiles are superposed. As is obvious from the figure, the magnitude of the maximum quadrupole splitting in the presence of Chol is almost identical for both hydrocarbon chains, thus suggesting no specific preference for Chol in either chain. This seems consistent with the aforementioned finding that no specific interaction existed between SM and Chol.

Another intriguing finding from Figure 4 is that the quadrupole splittings of the sphingosine chain from C8 to C16 nicely overlap with those of the acyl chain from C6' to C14'. A less obvious but similar tendency can be seen in sterol-free SSM membranes (Figure S5). Assuming that the deuterated methylenes at the same depth have identical quadrupole splittings irrespective of acyl or sphingosine chain,

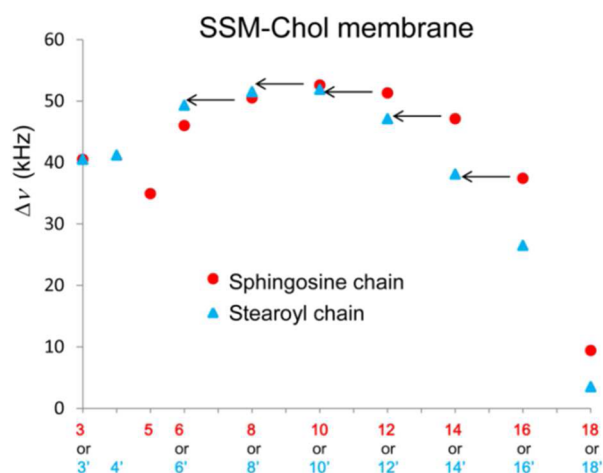


**Figure 4.** Comparison of quadrupole splitting profiles between sphingosine and stearyl chains for SSM–Chol membrane. Arrows indicate that the quadrupole splitting profile of the sphingosine chain (C8–C16) overlaps well with that of the acyl chain (C6'–C14'). This suggests that the acyl and sphingosine chains are mismatched by two methylene lengths.

this finding may suggest that acyl and sphingosine chains have a mismatch of about two methylene units. Indeed, the methyl group in the acyl chain (C18') has smaller quadrupole splittings than that in the sphingosine chain (C18) (Figure 2), indicating higher flexibility for the methyl group in the acyl chain due to the chain-length mismatch. Recently, we reported the conformation of the polar region of SSM in bicelles,<sup>15</sup> which is also reasonably consistent with a two-carbon chain-length mismatch. Of course, it is necessary to verify the above two-carbon-mismatch assumption using other methods such as neutron diffraction experiments, and for that purpose these site-specifically deuterated SSMs will be of great use.

#### Temperature Dependency of Quadrupole Splittings.

Because the phase transition temperature of a pure SSM membrane is 44 °C,<sup>16</sup> the measurements were carried out only at 45 and 50 °C in the absence of Chol, while in the presence of Chol, the quadrupole splittings were measurable even at 20 °C (Figure 5 and Tables S1–S19). As is evident from Figure 5, the quadrupole splitting values of the acyl chain in SSM membranes are significantly reduced with a temperature rise of only 5 °C from 45 to 50 °C, whereas only a small decrease occurs in the values for the SSM–Chol system with a temperature change of 30 °C from 20 to 50 °C. This also applies to the sphingosine chain (Figure S6). The smaller temperature sensitivity of the SSM–Chol membranes is attributable to the tighter packing in the liquid-ordered phase. Of note is the fact that the quadrupole splittings in the upper region (C2' and C3') are relatively less temperature-sensitive than those in the lower positions in both the presence and absence of Chol (Figure 5). This tendency is also clearly seen in the sphingosine chain (Figure S6). This can be accounted for by the aforementioned intermolecular hydrogen bonds among SM molecules; the occurrence of the intermolecular hydrogen bond is likely to provide higher temperature stability to the upper regions of SSM bilayers in both the presence and absence of Chol. More specifically, temperature dependence of quadrupole splitting may be accounted for by population change between trans and gauche conformations. The smaller temperature dependency in the upper region indicates that population is not changed by temperature rise because the

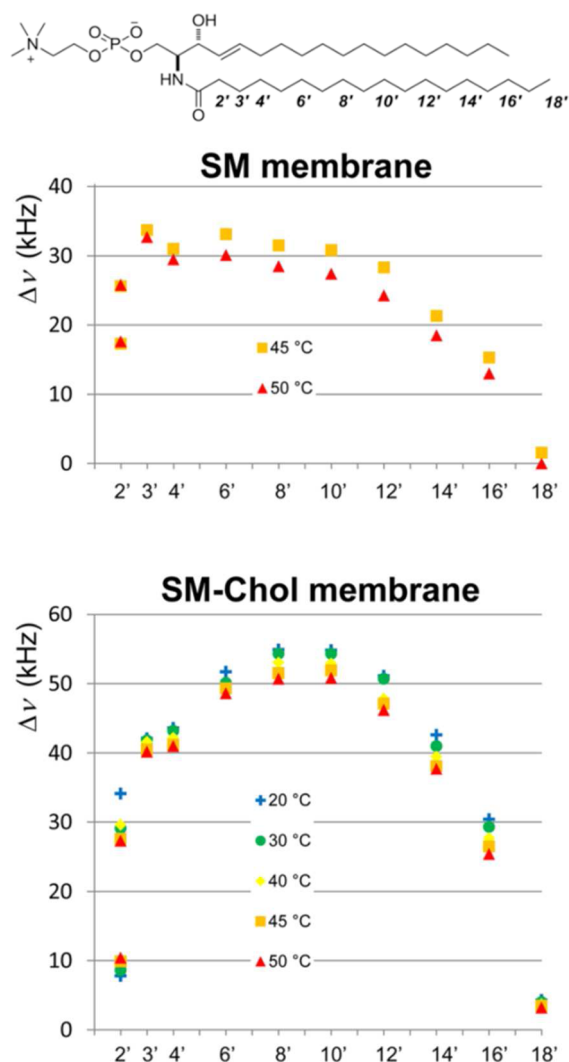


**Figure 5.** Temperature dependency of quadrupole splittings of the acyl chain of SSM. The upper region of the chain generally shows less temperature dependency than lower regions in both the presence and absence of Chol. This tendency is observed in the sphingosine chain (see Figure S6).

orientation of the amide portion is relatively fixed by the intermolecular hydrogen bonds. On the other hand, in the middle and lower chain, the temperature rise would increase the space between SM molecules or between SM and Chol (in other words, packing becomes looser) and enhance the gauche population, which may result in the larger temperature dependency.

**Implications for Raft Studies.** This study suggests that Chol is located more deeply in SM than in DMPC bilayers (Figure 6), which probably gives rise to the umbrella effect. The other findings are summarized as follows: (i) the C2'–C3' bond predominantly takes the gauche conformation, (ii) the net ordering effect of Chol in SM bilayers is not larger than that in PC bilayers, (iii) Chol has no specific preference for the acyl or sphingosine chain, (iv) the acyl and sphingosine chains seem mismatched by about two methylene length, and (v) the motion of the upper regions of SM chains is less temperature dependent than that of lower regions probably due to intermolecular hydrogen bond formation among SM molecules (Figure 6). Accordingly, the principal function of Chol in raft formation is, rather than specific interaction with SM,

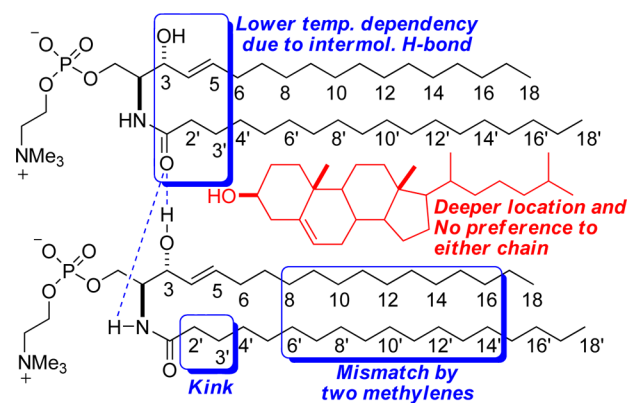


**Figure 6.** Schematic presentation of the results obtained in this study.

enhancement of the order in the middle portions of both sphingosine and acyl chains. A plausible scenario for raft formation, therefore, is that the thus-ordered hydrocarbon chains enable intermolecular van der Waals contacts between SM molecules and facilitate the formation of intermolecular hydrogen bond network between SM molecules, which would stabilize the liquid-ordered phase of SM membranes more than that of PC membranes. The intermolecular hydrogen bond network probably anchors Chol downward.

As described above, the characteristic order profiles of SM and their temperature dependency are not available without our comprehensive and selective deuteration strategy; in fact, previous studies that used SMs bearing perdeuterated acyl chains provided different quadrupole splitting profiles.<sup>2,3,21</sup> In addition, the present data may serve as a standard for future molecular dynamics studies of SM membranes since our quadrupole splitting profiles are more or less different from order profiles from a considerable number of simulation studies that have been conducted so far.<sup>27,30,32,34–38</sup>

## CONCLUSIONS AND FUTURE PROSPECTS

In this study, we have achieved comprehensive molecular motion capture of SM, one of the most important constituents in lipid rafts, by the combination of elaborate organic synthesis and NMR experiments. The order profiles presented here provided a reasonable model for the mechanism of raft formation; Chol enhances orders of the middle parts of SM hydrocarbon chains and facilitates intermolecular van der Waals contacts between SM molecules, leading to the formation of intermolecular hydrogen bond network among SM molecules, which would not only stabilize the liquid-ordered phase of SM membranes but also anchor Chol downward.

In future, application of these selectively deuterated SMs can be extended to a wide range of raft studies: SM dynamics in ternary or more complex membrane systems, the effects of peptides and proteins on SM membrane, and differences in ordering effects between Chol and other sterols. Moreover, selectively deuterated SMs can be feasibly applied to infrared and neutron diffraction experiments. It is also possible to extend this technique to ceramides and glycosyl ceramides, both of which are key players in lipid rafts. Indeed, these studies are currently underway in our group. We are firmly convinced that such comprehensively and site-selectively deuterated lipid molecules are a powerful and critical tool to scrutinize membrane dynamics at the atomic level and consequently to provide deeper understanding of biological membranes.



## ■ ASSOCIATED CONTENT

### ■ Supporting Information

Discussion on the depth of cholesterol in DMPC and SSM bilayers, comparison of quadrupole splitting profiles between sphingosine and stearoyl chains for SSM membrane, temperature dependency of quadrupole splittings of the sphingosine chain of SSM, tables of quadrupole splittings, and experimental procedures of synthesis. This material is available free of charge via the Internet at <http://pubs.acs.org>.

## ■ AUTHOR INFORMATION

### Corresponding Author

\*Phone (+81)-6-6850-5790, Fax (+81)-6-6850-5789, e-mail [matsmori@chem.sci.osaka-u.ac.jp](mailto:matsmori@chem.sci.osaka-u.ac.jp) (N.M.). Phone (+81)-6-6850-5774, Fax (+81)-6-6850-5774, e-mail [murata@chem.sci.osaka-u.ac.jp](mailto:murata@chem.sci.osaka-u.ac.jp) (M.M.).

### Funding

This work is supported by Grants-in-Aid for Scientific Research (S) (No. 18101010), for Priority Area (A) (No. 16073211) and (B) (No. 17681027) from MEXT, Japan, and a grant from Suntory Institute for Bioorganic Research, Japan; and also in part as ERATO "Lipid Active Structure Project" from Japan Science and Technology Agency (JST).

### Notes

The authors declare no competing financial interest.

## ■ ACKNOWLEDGMENTS

We thank Drs. Yuichi Umegawa and Naoya Inazumi in our department for help with  $^2\text{H}$  NMR measurements.

## ■ ABBREVIATIONS

SM, sphingomyelin; SSM, *N*-stearoylsphingomyelin; Chol, cholesterol; PC, phosphatidylcholine; PSPC, 1-palmitoyl-2-stearoyl-*sn*-glycero-3-phosphocholine; DMPC, 1,2-dimyristoyl-*sn*-glycero-3-phosphocholine; NMR, nuclear magnetic resonance.

## ■ REFERENCES

- (1) Seelig, J. (1977) Deuterium magnetic resonance: theory and application to lipid membranes. *Q. Rev. Biophys.* 10, 353–418.
- (2) Mehnert, T., Jacob, K., Bittman, R., and Beyer, K. (2006) Structure and lipid interaction of *N*-palmitoylsphingomyelin in bilayer membranes as revealed by  $^2\text{H}$ -NMR spectroscopy. *Biophys. J.* 90, 939–946.
- (3) Bartels, T., Lankalapalli, R. S., Bittman, R., Beyer, K., and Brown, M. F. (2008) Raftlike mixtures of sphingomyelin and cholesterol investigated by solid-state  $^2\text{H}$  NMR spectroscopy. *J. Am. Chem. Soc.* 130, 14521–14532.
- (4) Brown, M. F., and Chan, S. I. (1996) Bilayer membranes: deuterium & carbon-13 NMR, in *Encyclopedia of Nuclear Magnetic Resonance* (Gradt, D. M., and Harris, R. K., Eds.) Vol. 2, pp 871–885, Wiley, New York.
- (5) Calhoun, W. I., and Shipley, G. G. (1979) Fatty acid composition and thermal behavior of natural sphingomyelins. *Biochim. Biophys. Acta* 555, 436–441.
- (6) Simons, K., and Ikonen, E. (1997) Functional rafts in cell membranes. *Nature* 387, 569–572.
- (7) Byun, H. S., and Bittman, R. (2010) Selective deuterium labeling of the sphingoid backbone: facile syntheses of 3,4,5-trideuterio-d-erythro-sphingosine and 3-deuterio-D-erythro-sphingomyelin. *Chem. Phys. Lipids* 163, 809–813.
- (8) Matsumori, N., Okazaki, H., Nomura, K., and Murata, M. (2011) Fluorinated cholesterol retains domain-forming activity in sphingomyelin bilayers. *Chem. Phys. Lipids* 164, 401–408.

- (9) Davis, J. H., Jeffrey, K. R., Bloom, M., Valic, M. I., and Higgs, T. P. (1976) *Chem. Phys. Lett.* 42, 390–394.
- (10) Jungalwala, F. B., Hayssen, V., Pasquini, J. M., and McCluer, R. H. (1979) Separation of molecular species of sphingomyelin by reversed-phase high-performance liquid chromatography. *J. Lipid Res.* 20, 579–587.
- (11) Garner, A. E., Smith, D. A., and Hooper, N. M. (2007) Sphingomyelin chain length influences the distribution of GPI-anchored proteins in rafts in supported lipid bilayers. *Mol. Membr. Biol.* 24, 233–242.
- (12) Yamamoto, T., Hasegawa, H., Hakogi, T., and Katsumura, S. (2006) Versatile synthetic method for sphingolipids and functionalized sphingosine derivatives via olefin cross metathesis. *Org. Lett.* 8, 5569–5572.
- (13) Chandrakumar, N. S., and Hajdu, J. (1983) Stereospecific synthesis of ether phospholipids. preparation of 1-alkyl-2-(acylamino)-2-deoxyglycerophosphorylcholines. *J. Org. Chem.* 48, 1197–1202.
- (14) Dong, Z., and Butcher, J. A., Jr (1991) A useful synthesis of d-erythro-sphingomyelins. *Tetrahedron Lett.* 32, 5291–5294.
- (15) Yamaguchi, T., Suzuki, T., Yasuda, T., Oishi, T., Matsumori, N., and Murata, M. (2012) NMR-based conformational analysis of sphingomyelin in bicelles. *Bioorg. Med. Chem.* 20, 270–278.
- (16) Jaikishan, S., Bjoerkbom, A., and Slotte, J. P. (2010) Sphingomyelin analogs with branched *N*-acyl chains: The position of branching dramatically affects acyl chain order and sterol interactions in bilayer membranes. *Biochim. Biophys. Acta Biomembranes* 1798, 1987–1994.
- (17) Engel, A. K., and Cowburn, D. (1981) The origin of multiple quadrupole couplings in the deuterium NMR spectra of the 2 chain of 1,2 dipalmitoyl-*sn*-glycero-3-phosphorylcholine. *FEBS Lett.* 126, 169–171.
- (18) Cournia, Z., Ullmann, G. M., and Smith, J. C. (2007) Differential effects of cholesterol, ergosterol and lanosterol on a dipalmitoyl phosphatidylcholine membrane: a molecular dynamics simulation study. *J. Phys. Chem. B* 111, 1786–1801.
- (19) Mihailescu, M., Vaswani, R. G., Jardón-Valadez, E., Castro-Román, F., Alfredo Freitas, J. A., Worcester, D. L., Chamberlin, A. R., Tobias, D. J., and White, S. H. A. (2011) Acyl-chain methyl distributions of liquid-ordered and -disordered membranes. *Biophys. J.* 100, 1455–1462.
- (20) Silvius, J. R. (2003) Role of cholesterol in lipid raft formation: lessons from lipid model systems. *Biochim. Biophys. Acta* 1610, 174–183.
- (21) Bunge, A., Müller, P., Stöckl, M., Herrmann, A., and Huster, D. (2008) Characterization of the ternary mixture of sphingomyelin, POPC, and cholesterol: support for an inhomogeneous lipid distribution at high temperatures. *Biophys. J.* 94, 2680–2690.
- (22) Oldfield, E., Meadows, M., Rice, D., and Jacobs, R. (1978) Spectroscopic studies of specifically deuterium labeled membrane systems. Nuclear magnetic resonance investigation of the effects of cholesterol in model systems. *Biochemistry* 17, 2727–2740.
- (23) Smondyrev, A. M., and Berkowitz, M. L. (2001) Effects of oxygenated sterol on phospholipid bilayer properties: a molecular dynamics simulation. *Chem. Phys. Lipids* 112, 31–39.
- (24) Needham, D., McIntosh, T. J., and Evans, E. (1988) Thermomechanical and transition properties of dimyristoylphosphatidylcholine/cholesterol bilayers. *Biochemistry* 27, 4668–4673.
- (25) Léonard, A., Escribe, C., Laguerre, M., Pebay-Peyroula, E., Néri, W., Pott, T., Katsaras, J., and Dufourc, E. J. (2001) Location of cholesterol in DMPC membranes. a comparative study by neutron diffraction and molecular mechanics simulation. *Langmuir* 17, 3019–2030.
- (26) Maulik, P. R., and Shipley, G. G. (1996) Interactions of *N*-stearoyl sphingomyelin with cholesterol and dipalmitoylphosphatidylcholine in bilayer membranes. *Biophys. J.* 70, 2256–2265.
- (27) Róg, T., and Pasenkiewicz-Gierula, M. (2006) Cholesterol-sphingomyelin interactions: a molecular dynamics simulation study. *Biophys. J.* 91, 3756–3767.



- (28) Huang, J., and Feigenson, G. W. (1999) A microscopic interaction model of maximum solubility of cholesterol in lipid bilayers. *Biophys. J.* 76, 2142–2157.
- (29) Ohvo, H., and Slotte, J. P. (1996) Cyclodextrin-mediated removal of sterols from monolayers: effects of sterol structure and phospholipids on desorption rate. *Biochemistry* 35, 8018–8024.
- (30) Niemelä, P. S., Hyvönen, M. T., and Vattulainen, I. (2009) Atom-scale molecular interactions in lipid raft mixtures. *Biochim. Biophys. Acta* 1788, 122–135.
- (31) Janosi, L., and Gorfe, A. (2010) Importance of the sphingosine base double-bond geometry for the structural and thermodynamic properties of sphingomyelin bilayers. *Biophys. J.* 99, 2957–2966.
- (32) Zidar, J., Merzel, F., Hodoscek, M., Rebolj, K., Sepčić, K., Macek, P., and Janežic, D. (2009) Liquid-ordered phase formation in cholesterol/sphingomyelin bilayers: all-atom molecular dynamics simulations. *J. Phys. Chem. B* 113, 15795–15802.
- (33) Holopainen, J. M., Metso, A. J., Mattila, J., Jutila, A., and Kinnunen, P. K. J. (2004) Evidence for the lack of a specific interaction between cholesterol and sphingomyelin. *Biophys. J.* 86, 1510–1520.
- (34) Pandit, S. A., Vasudevan, S., Chiu, S. W., Mashl, R. J., Jakobsson, E., and Scott, H. L. (2004) Sphingomyelin-cholesterol domains in phospholipid membranes: atomistic simulation. *Biophys. J.* 87, 1092–1100.
- (35) Khelashvili, G. A., and Scott, H. L. (2004) Combined Monte Carlo and molecular dynamics simulation of hydrated 18:0 sphingomyelin-cholesterol lipid bilayers. *J. Chem. Phys.* 120, 9841–9847.
- (36) Niemelä, P. S., Hyvönen, M. T., and Vattulainen, I. (2006) Influence of chain length and unsaturation on sphingomyelin bilayers. *Biophys. J.* 90, 851–863.
- (37) Zhang, Z., Bhide, S. Y., and Berkowitz, M. L. (2007) Molecular dynamics simulations of bilayers containing mixtures of sphingomyelin with cholesterol and phosphatidylcholine with cholesterol. *J. Phys. Chem. B* 111, 12888–12897.
- (38) Hyvönen, M. T., and Kovanen, T. T. (2003) Molecular dynamics simulation of sphingomyelin bilayer. *J. Phys. Chem. B* 107, 9102–9108.